Journal of Nuclear Materials 450 (2014) 287–291

Contents lists available at ScienceDirect

Journal of Nuclear Materials

journal homepage: www.elsevier.com/locate/jnucmat

Solution enthalpy of Po and Te in solid lead–bismuth eutectic

Kim Rijpstra [a], Andy Van Yperen-De Deyne [a], Jörg Neuhausen [b], Veronique Van Speybroeck [a], Stefaan Cottenier [a,c,*]

[a] Center for Molecular Modeling, Ghent University, Technologiepark 903, BE-9052 Zwijnaarde, Belgium
[b] Laboratory for Radio- and Environmental Chemistry, Paul Scherrer Institute, OFLB/101, CH-5232 Villigen PSI, Switzerland
[c] Department of Materials Science and Engineering, Ghent University, Technologiepark 903, BE-9052 Zwijnaarde, Belgium

HIGHLIGHTS

- First-principles calculations can help planning difficult experiments with ^{210}Po.
- Po and Te do not dissolve into the bulk matrix of solid LBE.
- Formation of rock salt PbPo and PbTe is more exothermic than dissolution in bulk.
- Te-behaviour is predictive for Po-behaviour.
- Relativistic effects lead to a less negative solution enthalpy of Po in LBE.

GRAPHICAL ABSTRACT

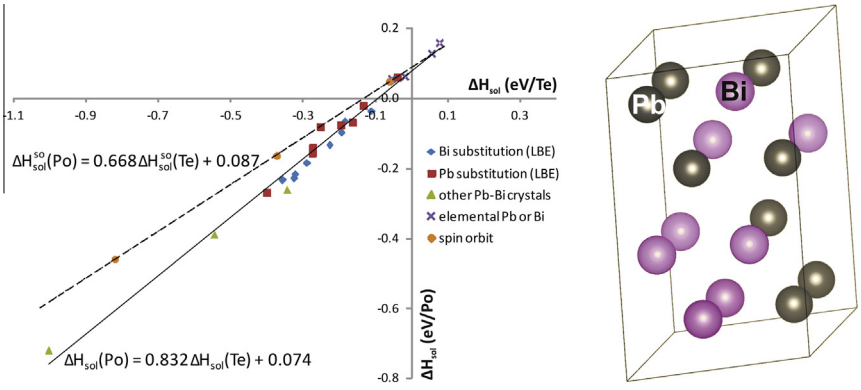

ARTICLE INFO

Article history:
Available online 11 July 2013

ABSTRACT

It is examined to which extent first-principles calculations can be used to collect *a priori* information on the solution enthalpy and solubility of Po in solid lead–bismuth eutectic (LBE). Such information can be helpful to limit the number of complicated experiments that are required to measure these properties. It is found that in the thermodynamic limit and at 0 K, Po does not dissolve in solid LBE. Its solution enthalpy is negative, in particular in Pb-rich environments, but competing compound-forming reactions are more exothermic. A clear correlation is found between the calculated solution enthalpies for Te in LBE and for Po in LBE, suggesting that Te-experiments can be used to map the expected behaviour for Po. The role of spin–orbit coupling as the major relativistic effect on the solution enthalpies of these heavy atoms is inspected.

© 2013 Elsevier B.V. All rights reserved.

1. Introduction

The molten phase of a lead–bismuth eutectic (LBE) is going to be used as coolant in planned experimental generation IV fission reactors [1]. Neutron capture by ^{209}Bi will inevitably lead to the presence of a non-negligible amount of radiotoxic ^{210}Po in the coolant. For safety assessments, it is essential to know how this Po will interact with its environment in several operation and accident scenarios. Eventually, this has to be examined experimentally. However, exactly due to its radiotoxicity, Po-experiments are subject to major safety constraints and are therefore not straightforward to perform. In order to minimize the number of experiments, it would be convenient to know in advance as well as possible what to expect. This is a situation where predictive computational modelling can play a role. Indeed, it is well-established that many properties of molecules [2] and solids [3–5] can be predicted by solving the fundamental equations provided by quantum physics. In the case of solids, this is most often done in the framework of Density Functional Theory (DFT). The solution enthalpy of impurity elements in metals is one example of a prop-

* Corresponding author at: Center for Molecular Modeling, Ghent University, Technologiepark 903, BE-9052 Zwijnaarde, Belgium. Tel.: +32 92646563.
E-mail address: Stefaan.Cottenier@ugent.be (S. Cottenier).

0022-3115/$ - see front matter © 2013 Elsevier B.V. All rights reserved.
http://dx.doi.org/10.1016/j.jnucmat.2013.07.004

erty that can be determined by DFT [6–12]. In this work, we will address the solution enthalpy of Po in solid LBE. We will do this in two ways: by directly predicting the solution enthalpy of a Po atom in solid LBE, and indirectly by dissolving the same amount of Te in exactly the same LBE-environment. The latter 'virtual experiment' will reveal a correlation between Po- and Te-behaviour, suggesting that it is possible to obtain information on Po in LBE by performing experiments on Te in LBE.

2. Computational details

All calculations in this work were done within the framework of Density Functional Theory [13–16], using the Perdew–Burke–Ernzerhof exchange–correlation functional [17]. The numerical method used to solve the scalar-relativistic [18] Kohn–Sham equations for periodic solids is the Projector Augmented Wave (PAW) method [19,20] as implemented in the VASP package [21,3] (6-electron PAW potential for Te, d-electrons included for Pb, Bi and Po). Spin–orbit coupling as the major relativistic effect beyond the scalar-relativistic level was added for the calculations described in Section 5. The cut-off energy for the basis set size was taken to be 290 eV. The k-grids were Γ-centered Monkhorst–Pack grids, with a density of 125,000 k-points/Å^{-3}. Both basis set size and k-point density were tested for numerical convergence. All unit cells were fully relaxed under the constraint of zero applied pressure and all calculated energies therefore correspond to enthalpies. No entropic effects were taken into account, such that all quantities refer to the ground state (0 K). The calculations reported in this paper are equivalent to 10 cpu-years of single-core computing.

3. Elemental solids and LBE-model

Five solids will play a major role in this work: the elemental solids Te, Pb, Bi and Po, and a Pb-Bi mixture. In order to demonstrate the validity of the computational method for this kind of solids, we list in Table 1 some predicted basic structural properties for the elemental solids. The computational settings as described in Section 2 were used. The bare calculated results were corrected for a systematic deviation as described in Ref. [5], and also the error estimates (1σ standard deviations) were taken from the latter work. The agreement between calculated and experimental values is reassuring for the validity of this computational method for this kind of solids. Furthermore, Table 1 demonstrates that spin–orbit coupling has a non-negligible effect on the properties of solids of heavy elements (see also Section 5).

Solid state DFT calculations require a unit cell as input, which is then periodically repeated to fill space. For an intrinsically disordered material as solid LBE, this straightforward approach is not possible. If it is the aim to describe the details of a disordered solid as faithfully as possible, one can resort to a set of elaborations or modifications of DFT that are meant for disordered alloys [22]: special quasi-random structures (SQS) [23], cluster expansion [24] or the coherent potential method (CPA) [25]. Our aim, however, is to inspect whether and how the local stoichiometry of the nearest-neighbour shell affects the solution behaviour of Po. We therefore take the simpler approach to describe a Pb–Bi alloy by a 'disordered supercell'. A unit cell of the underlying high-symmetry crystal structure is multiplied by a small integer factor in all three dimensions (in our case $2 \times 2 \times 2$, see Fig. 1(a)), and all atom sites are randomly occupied by a predefined number of Pb and Bi atoms. Subsequently the shape and volume of the cell as well as the positions of the atoms are allowed to adjust themselves in order to adopt the lowest-energy configuration under the condition of no applied pressure [12]. Applying the same procedure to a $3 \times 3 \times 3$ cell would require 100 times more computation time, and – as will be argued in Section 4 – is bound to lead to the same conclusions as are obtained from the $2 \times 2 \times 2$ cell. For the same reason, only one random choice of the Pb/Bi-occupation is considered (see Section 4).

Which underlying crystal structure has to be taken for LBE? A glance at the Pb–Bi phase diagram in Fig. 2 shows the relevant ones. Elemental Pb has the fcc structure (cF4, Cu-type), and elemental Bi has a rhombohedral structure (hR6, As-type). Around the concentration range of 70% Pb, the Pb–Bi mixture adopts the

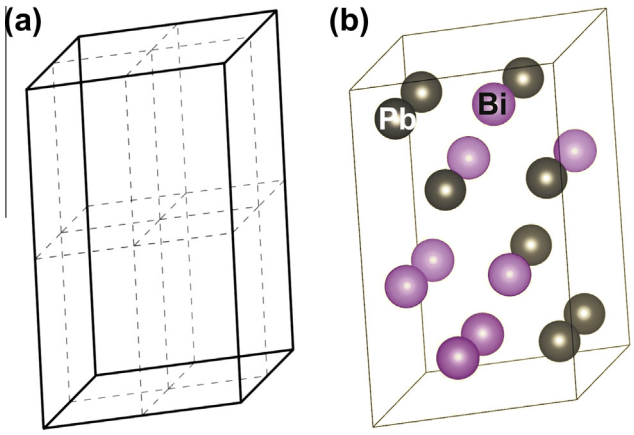

Fig. 1. (a) A $2 \times 2 \times 2$ supercell of the hexagonal close packed primitive cell. (b) The randomly chosen Pb- and Bi-occupation that served as a model for a configurationally disordered Pb/Bi-alloy in this work.

Table 1
Equilibrium volume per atom (Å^3) and equilibrium bulk modulus (GPa) for the bulk phases of Te, Pb, Bi and Po: experimental values (as listed in [5], extrapolated to 0 K and corrected for zero point motion), and calculated values (using the methods and settings described in Section 2) without (no SO) and with (SO) spin–orbit coupling. The calculated values have been corrected for the systematic deviations introduced by the PBE functional and an estimate of the expected uncertainty on the calculated value is given (see Ref. [5] for the procedure). Without spin–orbit coupling, all calculated volumes and bulk moduli agree with experiment within the error bar on the computed value, except for the bulk modulus of Po. When spin–orbit coupling is added, the latter disagreement is repaired.

	V_0 (Å^3/atom)			B_0 (GPa)		
	Exp.	no SO	SO	Exp.	no SO	SO
Te	33.30	33.70 (1.1)	–	26.2	18.7 (15)	–
Pb	29.86	30.86 (1.1)	31.03 (1.1)	46.3	41.9 (15)	38.1 (15)
Bi	35.13	35.62 (1.1)	36.85 (1.1)	32.1	27.3 (15)	24.3 (15)
Po	36.93	36.16 (1.1)	38.04 (1.1)	27.4	48.2 (15)	37.3 (15)

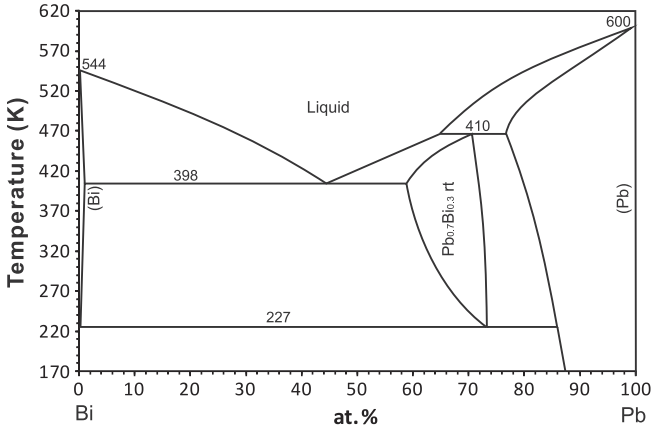

Fig. 2. The Pb–Bi phase diagram as given in Ref. [26] (picture redrawn from AtomWork [27,28]).

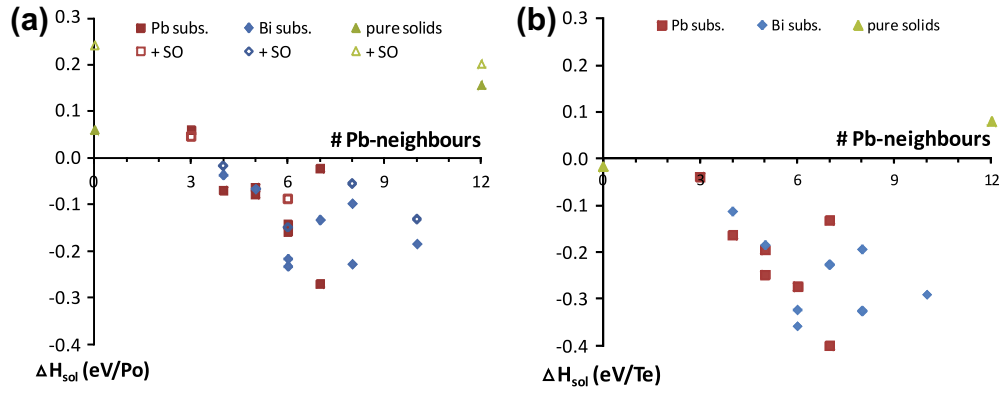

Fig. 3. (a) Solution enthalpy for Po at all 16 positions in our LBE model, as well as in pure Bi and pure Pb. These solution enthalpies are plotted with respect to the number of Pb-neighbours in the first coordination shell of Po. Open symbols are data points for which spin–orbit coupling has been taken into account. (b) Idem, but for Te instead of Po.

hcp structure (hP2, Mg-type). This hcp phase has a rather large homogeneity range. The solubility range of Pb in rhombohedral Bi is much smaller. In the broad concentration range between 1 at.% and 57 at.% Pb, the material will consist of a mixture of almost pure Bi microcrystals and hcp $Pb_{0.7}Bi_{0.3}$ microcrystals. Dissolving Po in LBE therefore means dissolving it in almost pure Bi and in hcp $Pb_{0.7}Bi_{0.3}$ (grain boundary effects are neglected). We want to examine how Po interacts with its immediate environment in Pb–Bi alloys. In order to sample as much as possible different nearest neighbour environments in a relatively small supercell, we take as our model system hcp-Pb_8Bi_8. This means: 8 Pb-atoms and 8 Bi atoms are randomly distributed over the 16 sites in a $2 \times 2 \times 2$ hcp supercell (Fig. 1(b)).

4. Dissolving Po and Te in LBE

How much energy does it cost to put one Po atom in (the Pb–Bi microcrysals of) a LBE matrix? To answer this, we examine the reaction

$$\underbrace{Pb_8Bi_8}_{\text{LBE}} + Po^{\text{solid}} \leftrightarrow \underbrace{Pb_8Bi_7Po}_{\text{LBE+Po}} + Bi^{\text{solid}} \tag{1}$$

which describes solid Po (α-Po, simple cubic) in contact with LBE (modelled by our 16-atom hexagonal cell), reacting to form solid bismuth and LBE with Po substituting for a Bi atom. A similar reaction can be written for Po substituting for Pb. The reaction enthalpy for Eq. (1) happens to be identical to the solution enthalpy of Po in LBE:

$$\Delta H^i_{\text{sol}} = \left[H(LBE + Po)_i + \mu_{\text{Pb(Bi)}}\right] - \left[H(LBE) + \mu_{\text{Po}}\right] \tag{2}$$

It expresses the total enthalpy cost to remove one Po-atom from a Po-reservoir with chemical potential μ_{Po}, to put it at a Pb (or Bi) site in LBE, and to bring the replaced Pb-atom (or Bi-atom) to a Pb-reservoir (or Bi-reservoir) with chemical potential μ_{Pb} (or μ_{Bi}). For the reservoirs (or chemical potentials μ), one usually takes the enthalpy per atom in the elemental solids, i.e. as determined by the calculations described in Section 3.

One after the other, all 16 Pb or Bi atoms in our model LBE are replaced by a Po atom, after which the supercell is allowed in all cases to relax completely. This results in 16 different values for the enthalpy $H(LBE + Po)_i$ ($1 \leqslant i \leqslant 16$). These 16 solution enthalpies are plotted in Fig. 3(a) as a function of the number of Pb atoms in the first coordination shell of Po. The same picture shows the solution enthalpy for Po in rhombohedral Bi and fcc-Pb as well. The solution enthalpy for Po in Pb is positive, indicating that at 0 K Po will not dissolve spontaneously in Pb. For Po in Bi, the (scalar-relativistic) solution enthalpy is slightly positive as well. For Po in LBE, there is a rough trend with respect to the number of Pb neighbours: Po has a positive solution enthalpy when it goes to sites with few Pb neighbours, and a negative solution enthalpy when it goes to sites with many Pb neighbours. This negative solution enthalpy means that the reaction in Eq. (1) will proceed exothermally to the right if Po ends up in an environment with a lot of Pb-atoms. It does not mean, however, that Po will effectively dissolve into the solid Pb/bi-microcrystals in LBE in Nature. For this to happen, there should be no alternative reaction that is even more exothermal. As solid PbPo is experimentally known to exist in the rocksalt structure [29], a straightforward alternative that should be examined is

$$\underbrace{Pb_8Bi_8}_{\text{LBE}} + Po^{\text{solid}} \leftrightarrow \underbrace{Pb_7Bi_7}_{\text{LBE}} + PbPo^{\text{solid}} + Bi^{\text{solid}} \tag{3}$$

The reaction enthalpy for this reaction is calculated to be −0.60 eV/Po, which is clearly lower than the lowest value of −0.27 eV/Po in Fig. 3(a) (or Eq. (1)). As a consequence, Po will not dissolve spontaneously into solid LBE.[1] Either it will react with LBE to form rocksalt PbPo and rhombohedral Bi, or it will follow other reaction paths that have even more negative reaction enthalpies (involving, for instance, ternary Pb–Bi–Po phases). This conclusion is consistent with experimental observations that Po inside solid Pb [30] and solid LBE [31,32] migrates to the surface and/or to grain boundaries [33].

Exactly the same procedure was followed to determine the solution enthalpy of Te in LBE. This results in Fig. 3(b) for a reaction similar to Eq. (1). The solution enthalpy for Te in solid Pb is positive, consistent with the low solubility range of Te in Pb [34]. At the Bi-side, the solution enthalpy is slightly negative. Yet, in low-temperature experiments Te will not dissolve in rhombohedral Bi, as it is more favourable to form Bi_4Te_3 [35]. This too is consistent with the low solubility range of Te in Bi (0.2 at.% at most [36]). The solution enthalpy of Te in the Pb/Bi-microcrystals of LBE is considerably negative (down to −0.40 eV/Te), and Te prefers Pb-rich environments in LBE, just as Po does. Te is not expected to dissolve effectively into LBE, however, as also here at least one competing reaction can be found with a lower reaction enthalpy: the analogue of Eq. (3) with PbTe has a reaction enthalpy of −0.96 eV/Te. PbTe is indeed the phase that is found experimentally [37–39].

At this point, one can exploit a particular feature of first principles calculations: the ability to do very controlled ‘experiments’ in

[1] As −0.60 eV is considerably lower than −0.27 eV, this conclusion will not be affected by taking a different random occupation for the 16-atom LBE cell, or by taking a larger supercell to model LBE.

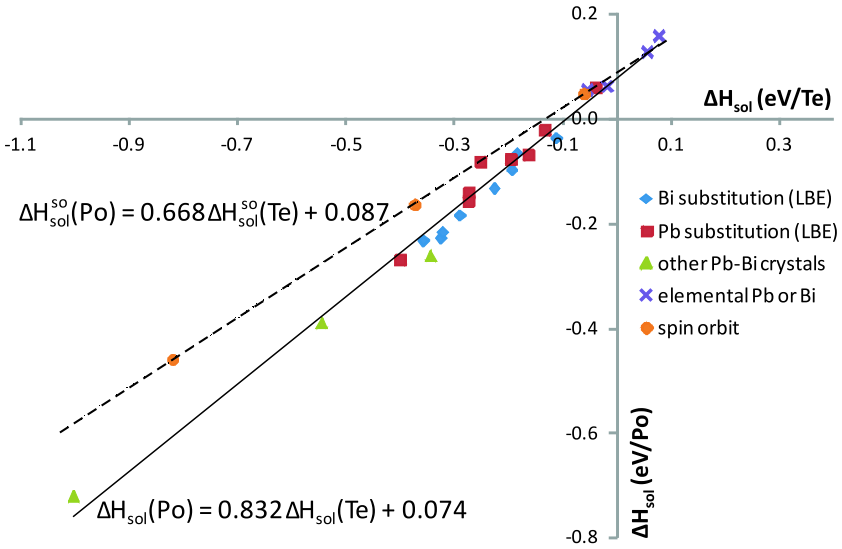

Fig. 4. Correlation between the solution enthalpies of Po and Te in LBE (1/16), elemental Pb (various concentrations), and in elemental Bi (1/24). Additionally, the same correlation for full subsitution of either Pb or Bi by Po or Te is given for PbBi (NaCl-structure) and for Bi_4Pb_3. Every data point corresponds to a different local environment for Po/Te. In the two calculations that lead to every data point, all atomic positions were independently optimized (=the distance between Te and its neighbours is allowed to be different from the distance between Po and its neighbours). The dashed line is a similar fit through three well-separated data points, now taking spin–orbit coupling into account (from left to right: Bi-substitution in PbBi [NaCl], Pb-substitution in PbBi [NaCl], 25% of Po/Te in fcc-Pb).

a way that is not achievable in a lab. Using the 2×18 data points in both Fig. 3(a) and (b), we can compare the enthalpy cost of putting either Po or Te in *the same* atomistic environment (i.e. identical coordination symmetry, different bond lenghts). If these two data sets are plotted with respect to each other, an excellent linear correlation emerges (Fig. 4). In order to test whether or not this correlation depends on the particular $2 \times 2 \times 2$ LBE-model we have chosen, data points for reaction enthalpies of other crystals in contact with solid Te or solid Po were calculated: Te/Po as impurity in fcc Pb (concentrations of 3.1%, 6.25% and 25%), Te/Po as impurity in rhombohedral Bi (4.2%), substitution of all Pb in hypothetical Bi_4Pb_3 by Te/Po, and substitution of either all Pb or all Bi in hypothetical rocksalt PbBi by Te/Po. As Fig. 4 shows, these data points obtained in very different crystals perfectly follow the linear correlation. This strongly suggests that this linear correlation is a genuine property, and not an artefact due to the limited $2 \times 2 \times 2$ LBE supercell or the single random configuration. The linear correlation in Fig. 4 implies that Te is more strongly bound to the LBE matrix than Po is: environments that bind Te by less than 0.09 eV per solute atom, do not bind Po any longer (less than 0.14 eV per solute atom if spin–orbit coupling is considered). The latter is consistent with experimental observations in solid PbTe and solid PbPo (rock salt structure): whereas PbTe melts at 1195 K [40], PbPo decomposes already between 820 and 900 K [41,42] or sublimes around 1000 K [29]. Another corroborating observation is the evaporation rate of Po from LBE, which is larger than the one of Te from LBE [43].

Knowing this correlation, it would be possible to predict the solution enthalpy of Po in any LBE-like environment without making a DFT calculation, provided one has calculated the solution enthalpy of Te in that same environment. By extension, this applies to experiment as well: performing experiments on Te in LBE provides information that in principle could be translated to Po in LBE.

5. Influence of spin–orbit coupling

The common way to perform DFT calculations is to do it at the scalar-relativistic level [18]. This includes, for instance, the speed dependence of the mass of the electron. For heavy atoms, relativistic effects beyond the scalar-relativistic level cannot be entirely neglected. The dominant effect is spin–orbit coupling, which can be added in a perturbative way to scalar-relativistic calculations. Table 1 demonstrates the impact of spin–orbit coupling on the equilibrium volume and bulk modulus of the pure phases of Pb, Bi and Po: without spin–orbit coupling, all calculated volumes and bulk moduli agree with experiment within the error bar on the computed value, except for the bulk modulus of Po. When spin–orbit coupling is added, the latter disagreement is repaired. Therefore, we did apply spin–orbit coupling to some of the Po-substitutions in LBE. The result is that the scalar-relativistic solution enthalpies are shifted in the direction of more positive values by a varying amount, that has the order of magnitude of 0.1 eV per solute atom (open symbols in Fig. 3(a)). This shows that the Po solution enthalpy is less negative than the scalar-relativistic calculations suggested. However, the qualitative conclusions are not affected (no dissolution in the pure materials, Pb-rich environments preferred in LBE). For three well-separated points in Fig. 4, all calculations were repeated with spin–orbit coupling (including the geometry optimization). This allows to determine the linear correlation with spin–orbit coupling taken into account (dashed line in Fig. 4). It is this line which should be used to convert experimental solution enthalpies for Te into predicted solution enthalpies for Po.

6. Conclusions

Starting from a simple model system for solid LBE and using only information obtained from first-principles calculations, we predict that at low temperatures Po will not dissolve in the matrix of solid LBE (grain boundary solution was not studied). Although its solution enthalpy is negative (and most so in Pb-rich environments), competing compound-forming reactions are more exothermic. Similar calculations for Te in LBE show that Te is bound stronger by the LBE matrix than Po is. Solution enthalpies for Te in LBE correlate strongly with solution enthalpies for Po in LBE. This suggests that Te experiments can be used to map the expected behaviour for Po, a procedure that can reduce the number of required Po experiments.

Acknowledgements

This work is supported by the European Commission through the FP7 project SEARCH (Safe ExploitAtion Related CHemistry for HLM reactors, Project Nr. 295736) and by the Research Board of Ghent University. The authors acknowledge helpful discussions with Alexander Aerts (SCK-CEN, Mol), Emilio Andrea Maugeri and Matthias Rizzi (both PSI, Villigen). Three anonymous referees have contributed valuable suggestions. Stefaan Cottenier acknowledges financial support from OCAS NV by an OCAS-endowed chair at Ghent University. Calculations were carried out using the Stevin Supercomputer Infrastructure at Ghent University, funded by Ghent University, the Hercules Foundation, and the Flemish Government (EWI Department).

References

[1] H.A. Abderrahim, P. Baeten, D. De Bruyn, R. Fernandez, Energy Conversion and Management 63 (2012) 4–10.
[2] Pekka Pyykkö, John F. Stanton (Eds.), Chemical Reviews 112 (2012) 1–672.
[3] J. Hafner, Journal of Computational Chemistry 29 (2008) 2044.
[4] K. Schwarz, P. Blaha, S. Trickey, Molecular Physics 108 (2010) 3147.
[5] K. Lejaeghere, V. Van Speybroeck, G. Van Oost, S. Cottenier, Critical Reviews in Solid State Physics and Materials Science 39 (2014) 1.
[6] D. Jiang, E.A. Carter, Physical Review B 67 (2003) 214103.
[7] C. Wolverton, V. Ozolins, M. Asta, Physical Review B 69 (2004) 144109.
[8] C. Wolverton, V. Ozolins, Physical Review B 73 (2006) 144104.
[9] F. Soisson, C. Fu, Physical Review B 76 (2007) 214102.
[10] P. Erhart, B. Sadigh, A. Caro, Applied Physics Letters 92 (2008) 141904.
[11] A. Harutyunyan, N. Awasthi, A. Jiang, W. Setyawan, E. Mora, T. Tokune, K. Bolton, S. Curtarolo, Physical Review Letters 100 (2008) 195502.
[12] K. Lejaeghere, S. Cottenier, S. Claessens, M. Waroquier, V.V. Speybroeck, Physical Review B 83 (2011) 184201.
[13] P. Hohenberg, W. Kohn, Physical Review 136 (1964) B864.
[14] W. Kohn, L.J. Sham, Physical Review 140 (1965) A1133.
[15] R. Martin, Electronic Structure, Basic Theory and Practical Methods, Cambridge University Press, 2004.
[16] S. Cottenier, Density Functional Theory and the Family of (L)APW-Methods: A Step-By-Step Introduction, (Instituut voor Kern- en Stralingsfysica, KULeuven, Belgium), 2002. <http://www.wien2k.at/reg_user/textbooks> (ISBN: 90-807215-1-4).
[17] J.P. Perdew, K. Burke, M. Ernzerhof, Physical Review Letters 77 (1996) 3865.
[18] D. Koelling, B. Harmon, Journal of Physics C: Solid State Physics 10 (1977) 3107.
[19] P.E. Blöchel, Physical Review B 50 (1994) 17953.
[20] G. Kresse, D. Joubert, Physical Review B 59 (1999) 1758.
[21] G. Kresse, J. Furthmüller, Physical Review B 54 (1996) 11169.
[22] M.H.F. Sluiter en, Y. Kawazoe, Europhysics Letters 57 (2002) 526–532.
[23] A. Zunger, S. Wei, L. Ferreira, J. Bernard, Physical Review Letters 65 (1990) 353–356.
[24] S. Müller, Journal of Physics: Condensed Matter 15 (2003) R1429.
[25] P.E.A. Turchi, M. Sluiter, F.J. Pinski, D.D. Johnson, D.M. Nicholson, G.M. Stocks, J.B. Staunton, Physical Review Letters 67 (1991) 1779–1782.
[26] T.B Massalski, H. Okamoto, P.R. Subramanian, L. Kacprzak, Binary Alloys Phase Diagrams, second ed., ASM International, 1990, pp. 772–773.
[27] National Institute for Materials Science (NIMS), AtomWork, 2012. <http://crystdb.nims.go.jp/>.
[28] Y. Xu, M. Yamazaki, P. Villars, Japanese Journal of Applied Physics 50 (2011) 11RH02.
[29] W. Witteman, A. Giorgi, D. Vier, Journal of Physical Chemistry 64 (1960) 434.
[30] A. Zastawny, J. Bialon, T. Sosinski, Applied Radiation and Isotopes 40 (1989) 19.
[31] T. Miura, T. Obara, H. Sekimoto, Applied Radiation and Isotopes 61 (2004) 1307.
[32] J. Neuhausen, D. Schumann, R. Dressler, B. Eichler, S. Heinitz, B. Hammer, F. von Rohr, L. Zanini, V. Boutellier, M. Rthi, J. Eikenberg, E. Noah, Proceedings of the DAE-BRNS Symposium on Nuclear and Radiochemistry NUCAR-2011, vol. 44, Visakhapatnam, 2011.
[33] G. Tammann, A. von Löwis of Menar, Zeitschrift für anorganische und allgemeine Chemie 205 (1932) 145.
[34] V. Kutznetsov, V. Zlomanov, Inorganic Materials 25 (1989) 923.
[35] K. Yamana, K. Kihara, T. Matsumoto, Acta Crystallographica B 35 (1979) 147.
[36] S. Chizhevskaya, L. Shelimova, V. Zemskov, V. Kosyakov, D. Malakhov, Inorganic Materials 30 (1994) 1.
[37] R. Blachnik, F. Romermann, A. Schlieper, Zeitschrift fur Metallkunde 88 (1997) 301.
[38] R. Oshea, J. Donovan, E. Peretti, Transactions of the Metallurgical Society of AIME 221 (1961) 1266.
[39] R. Oshea, E. Peretti, Transactions of the American Society of Metals Quarterly 56 (1963) 153.
[40] W. Gierlotka, J. Lapsa, D. Jendrzejczyk-Handzlik, Journal of Alloys and Compounds 479 (2009) 152.
[41] J. Goode, Mound Laboratory Report 1952/55; N.S.A. 10, 1956.
[42] T. Miura, T. Obara, H. Sekimoto, Annals of Nuclear Energy 34 (2007) 926.
[43] J. Neuhausen, U. Köster, B. Eichler, Radiochimica Acta 92 (2004) 917.